



Article

# Smart Thermomechanochemical Composite Materials Driven by Different Forms of Electromagnetic Radiation

Kevin Riberi, Silvestre Bongiovanni Abel , María V. Martínez, María A. Molina \* ,  
Claudia R. Rivarola, Diego F. Acevedo , Rebeca Rivero, Emma Antonia Cuello ,  
Romina Gramaglia and Cesar A. Barbero \*

Research Institute for Energy Technologies and Advanced Materials (IITEMA), National University of Río Cuarto (UNRC)-National Council of Scientific and Technical Research (CONICET), Ruta Nacional N° 36, Km 601, Río Cuarto (Córdoba) 5800, Argentina; kevinriber@gmail.com (K.R.); bongiovanniabel.s@gmail.com (S.B.A.); mmvictoriarmartinez@gmail.com (M.V.M.); crivarola@exa.unrc.edu.ar (C.R.R.); dacevedo@ing.unrc.edu.ar (D.F.A.); rebecaerivero@gmail.com (R.R.); emmantoniam.c@gmail.com (E.A.C.); rgramaglia@exa.unrc.edu.ar (R.G.)

\* Correspondence: mamolina7@gmail.com (M.A.M.); cesarbarbero@gmail.com (C.A.B.);  
Tel.: +54-358-467-6157 (M.A.M. & C.A.B.)

Received: 14 November 2019; Accepted: 20 December 2019; Published: 1 January 2020



**Abstract:** Photo-thermo-mechanochemical (P-T-MCh) nanocomposites provide a mechanical and/or chemical output (MCh) in response to a photonic (P) input, with the thermal (T) flux being the coupling factor. The nanocomposite combines a photon absorbing nanomaterial with a thermosensitive hydrogel matrix. Conjugated (absorbing in the near infrared (NIR, 750–850 nm) wavelength range) polymer (polyaniline, PANI) nanostructures are dispersed in cross-linked thermosensitive (poly(*N*-isopropylacrylamide), PNIPAM) hydrogel matrices, giving the nanocomposite P-T-MCh properties. Since PANI is a conductive polymer, electromagnetic radiation (ER) such as radiofrequency (30 kHz) and microwaves (2.4 GHz) could also be used as an input. The alternating electromagnetic field creates eddy currents in the PANI, which produces heat through the Joule effect. A new kind of “product” nanocomposite is then produced, where ER drives the mechanochemical properties of the material through thermal coupling (electromagnetic radiation thermomechanochemical, ER-T-MCh). Both optical absorption and conductivity of PANI depend on its oxidation and protonation state. Therefore, the ER-T-MCh materials are able to react to the surroundings properties (pH, redox potential) becoming a smart (electromagnetic radiation thermomechanochemical) (sER-T-MCh) material. The volume changes of the sER-T-MCh materials are reversible since the size and shape is recovered by cooling. No noticeable damage was observed after several cycles. The mechanical properties of the composite materials can be set by changing the hydrogel matrix. Four methods of material fabrication are described.

**Keywords:** electromagnetic radiation; smart materials; product composites; thermosensitive hydrogel; conducting polymer

## 1. Introduction

Composite materials are made of two materials, one dispersed in the other (called the matrix), which are present as two different phases [1]. In the case of nanocomposites, the dispersed component has at least one dimension in the nanometric range [2]. Usually, the properties of the dispersed material and that of the matrix combine to produce improved properties, which are the “sum” of the component properties. The properties of a composite material are determined by the properties

of the constituents, their volumetric participation, and the interaction among themselves and with the applied fields. Composites enhance one or more properties that are already available in both constituents, approximately according to the sum of the contributions from the constituents weighed by their volume fraction. In addition to the conventional fiber reinforced composites with better mechanical properties than fiber or matrix, other properties can be added (e.g., electronic conductivity, electromagnetic field isolation, optical absorption, hardness, erosion resistance, vibration damping, etc.) [3]. In the case of nanocomposites (e.g., nanoclays dispersed in a thermoplastic matrix), the combination of hard but fragile clay nanoplates and elastic thermoplastic matrix produces a material which is both flexible and tenacious [4].

However, there is a new type of composite that is able to generate a physical response that is completely absent from any of its constituents. For example, a non-conducting material can produce electricity when excited by a magnetic field, which is a peculiar response that neither of the two constituents (a piezoelectric and a magnetorestrictive phase) could produce alone. This new class of composites, termed “product” composites, opens up new possibilities for previously unimagined material responses [3]. In “sum” composites, if one component material loses its characteristic property, the composite material still retains the properties of the other component. On the other hand, in “product” composites, losing the property of one material implies the loss of the property for the whole nanocomposite. Such behavior makes it easy to modulate, or switch off/on, the nanocomposite property affecting the properties of only one component in a defined way. Moreover, in this way, the material reacts actively to external stimuli becoming a smart material. Van Suchtelen [5] described in detail the theory behind this kind of composite, differentiating the composites with “product” properties from the “sum” properties of conventional composites (e.g., fiber-reinforced composites). One known way to make a “product” nanocomposite is to disperse a photon-absorbing material in a thermosensitive matrix. In a general sense, electromagnetic radiation (ER) is the physical input, producing heat in the nanomaterial (ER-T-MCh). The heat is transferred by thermal conduction (T) to the hydrogel and induces the phase transition at a given temperature. The phase transition causes a volume change, which can be used as mechanical actuation (M). The gel also expels the inner solution [6], and the porous surface of the gel increases its hydrophobicity [7], producing a chemical output (Ch). Therefore, the phase transitions of the gel are fully reversible, and the initial volume will be restored upon cooling. The inner solution will be taken in as far as it remains in contact with the material. Under these conditions, the cycle can be performed several times without damage. Both effects represent chemical (Ch) effects. The resulting nanocomposite is an ER driven thermo-mechanical/chemical (ER-T-MCh) or photothermomechanicochemical (P-T-MCh) if only light is used as input. The thermosensitive matrix is usually a polymer cross-linked by covalent bonds (e.g., poly(*N*-isopropylacrylamide)) showing a lower critical solution temperature (LCST) [8]. The free chains, between crosslinks, are solvated in water in a coil state below the LCST. When the hydrogel is heated and the temperature reaches the LCST, a coil-to-globule transition occurs with hydrogel shrinking. The volume change (mechanical output) is accompanied by a hydrophilic to hydrophobic change of the gel surface (chemical output). Additionally, the swelling solution is expelled from the gel, allowing the release of molecules (e.g., a medicinal drug). The other kind of hydrogels used are those having non-covalent crosslinks (e.g., hydrogen bonding) that show a gel to sol transition at a given temperature. Among these are proteins (e.g., gelatin) and polysaccharides (e.g., agar) [9]. In this case, the gel dissolves upon heating allowing liberation of active principles or similar action. Direct far infrared radiation allows for remote heating, but cannot be used in the body because it is strongly absorbed by the tissue. On the other hand, near infrared (700–1200 nm) light is weakly absorbed in normal tissue but it is not absorbed in thermosensitive polymers. If a species (material or molecule) with strong near infrared absorption could be incorporated into the material, the absorbed radiation will be dissipated as heat triggering the coil to globule transition of the thermosensitive polymer, effectively giving the P-T-MCh property to the new material.

Several photon-absorbing materials have been used as NIR absorbers. The most widely used involve gold nano-objects. Gold nanorods have a longitudinal mode of the localized surface plasmon

resonance (LSPR) with strong absorption in the NIR (700–900 nm) range [10]. Therefore, it has been extensively used to produce materials with P-T-MCh properties [11]. Another metal nanostructure with strong plasmonic absorption in the near infrared region is gold nanoshells [12]. It has also been used to produce P-T-MCh nanocomposites. On the other hand, gold nanospheres show LSPR bands in the visible range (400–600 nm) [13], not in the near infrared range. Therefore, it has been used to produce P-T-MCh materials which are driven by light in the visible range [14]. However, Wu et al. used NIR radiation to heat gels loaded with aggregated gold nanoparticles, showing an almost constant absorbance up to 820 nm [15]. Since both the gold nanostructures and the hydrogel could be made by soft chemistry methods, the nanocomposite could be made by in situ formation of either component, together with the other preformed material. Magnetite ( $\text{Fe}_3\text{O}_4$ ) has been extensively heated up by alternating magnetic fields due to magnetostrictive effects [16]. However, magnetite also shows light absorption in the NIR range and several P-T-MCh nanocomposites have been built using this nanomaterial [17]. Several inorganic solids (e.g., CuS) show semiconducting properties that is to present a small band gap between the valence and conduction bands. The electrons in the valence band can be excited by light to the conduction band. The energy of the band gap usually falls in the visible-NIR range. Therefore, nanoparticles of several semiconducting inorganic materials have been used to build P-T-MCh nanocomposites [18]. Other materials used to absorb NIR in P-T-MCh materials are carbon nanomaterials. Since they have extended conjugation (e.g., carbon nanotubes (MWNT)), show multiple absorption bands covering the UV-visible-NIR range [19]. MWNT were incorporated into thermosensitive hydrogels and irradiated with NIR [20]. Graphene oxide nanoplates are also used as absorbing component in P-T-MCh nanocomposites [21]. Additionally, P-T-MCh materials could be made using other 2D materials, like  $\text{MoS}_2$  [22],  $\text{MoSe}_2$  [23], WN [24], and exfoliated black phosphor [25]. Highly conjugated molecules present a small gap between the highest occupied molecular orbital (HOMO) and the lowest unoccupied molecular orbital (LUMO). Therefore, the chromophores are absorbed in the NIR (700–1100 nm) region [26]. Surprisingly, few cases have reported the use of low molecular weight dyes to build P-T-MCh materials [27]. More common is the use of conjugated polymers, especially those of biological origin [28]. Conducting polymers have been used to act as light absorbers in P-T-MCh materials, either as absorber only [29] or combined with NIR dyes [30].

In the present article, a new kind of product material is described: smart electromagnetic radiation-driven thermo-mechanochemical (sER-T-MCh) nanocomposites. sER-T-MCh materials are made by combining a conducting polymer (polyaniline, PANI) nanostructures with a thermosensitive hydrogel (poly(*N*-isopropylacrylamide), PNIPAM). Since PANI absorbs light in the NIR region and is electrically conductive, the electromagnetic radiation input can be varied from NIR I light (750–850 nm) to microwaves (2.4 GHz) and oscillating electromagnetic fields (radiofrequency (RF), 30 kHz). Therefore, the P-T-MCh materials are a special case of ER-T-MCh materials. Smart, or stimuli-responsive, materials are able to dramatically change their volume and other properties (opacity, hydrophobicity, mechanical properties, etc.) in response to environmental stimuli [31]. The PANI component in ER-T-MCh materials changes optical absorption and conductivity with pH or redox potential of the solution, effectively modulating the ER absorption and heat release. Due to the “product” nature of the composite, the mechanochemical (MCh) output will then be modulated by the external stimuli (pH, redox potential). Therefore, the material will not act passively, like other P-T-MCh materials (e.g., gold nanorods), but react to changes in the media. Such “smartness” of PANI nanoparticles has been used to perform the selective ablation of tumor cells in the presence of normal cells based on the lower cytoplasmic pH of tumor cells compared with normal ones [32].

Four methods of fabrication are described: (i) INH infiltration of preformed conducting polymer nanoparticles inside porous hydrogels; (ii) GAN: gelation of the smart hydrogel matrix around the conductive polymer nanoparticles dispersed in the polymerization solution; (iii) PIH: in situ formation (by oxidative polymerization of a monomer) of the conductive polymer inside the hydrogel matrix;

and (iv) AMH: absorption of free conducting macromolecules inside the smart hydrogel matrix from their true solutions.

It is noteworthy that some of the P-T-MCh nanocomposites could be also driven by other electromagnetic radiation (making them ER-T-MCh). Both gold and carbon nanostructures present large electronic conductivities. However, to the best of our knowledge, no ER-T-MCh materials based on Au or C nanomaterials and driven by electromagnetic radiation (microwaves, radiofrequency) have been described.

## 2. Materials and Methods

Polyvinylpyrrolidone with Mw of 30.000 g/mol (PVP-30K) was obtained from Anedra (Buenos Aires, Argentina). Aniline (ANI, 99%), aniline hydrochloride (ANI-HCl, 98%) and ammonium persulfate (APS) were obtained from Sigma-Aldrich (St. Louis, MO, USA). *N*-isopropylacrylamide (NIPAM), 2-acrylamido-2-methyl-1-propanesulfonic acid (AMPS) and *N,N'* methylenebis(acrylamide) (BIS) were obtained from Scientific Polymer Products (Ontario, NY, USA). Pyrrole (Py) was obtained from Fluka (Buchs, Switzerland). All reactions were carried out in bidistilled water.

### 2.1. Polyaniline Solutions

Polyaniline (PANI) was synthesized by oxidative polymerization from a solution of ANI-HCl (0.2 M) in water, using APS (0.2 M) as the oxidant. Polymerization was carried out at room temperature for 60 min. The polymer was purified by filtering under vacuum and washing with 1 M HCl. The base form was prepared by stirring in  $\text{NH}_4\text{OH}$  (0.1 M) solution during 24 h. Then, the solid is filtered and dried under vacuum for 24 h, to produce PANI (emeraldine base form, PANI-EB).

PANI-EB solution in *N*-methylpyrrolidone (NMP) (1% p/v) was prepared by stirring the PANI-EB solid in NMP for 4 h. PANI (emeraldine salt form, PANI-ES) solution in  $\text{CHCl}_3$  (0.5% p/v) was prepared by stirring the PANI-EB solid in a 1 M solution of champhorsulfonic acid and filtering out the insoluble particles.

### 2.2. Polyaniline Copolymer: Polyaniline-*b*-poly(*N*-isopropylacrylamide) (PANI-*b*-PNIPAM)

The block copolymer of PNIPAM and PANI was synthesized in two steps. First, a PNIPAM telechelic chain terminated in aniline unit is obtained by free radical polymerization of NIPAM monomer, using an azo initiator, in the presence of a chain transfer agent (4-aminothiophenol, 4-ATF) to yield PNIPAM-ATF [33]. Then, the oxidative polymerization of aniline monomer was carried out with APS as oxidant. The PANI chains grow from the PNIPAM-S-C<sub>6</sub>H<sub>4</sub>-NH<sub>2</sub> extreme to produce a linear block copolymer (PNIPAM-*b*-PANI) [34].

### 2.3. Synthesis of Crosslinked Thermosensitive Hydrogels of Poly(*N*-isopropylacrylamide) (cPNIPAM)

#### 2.3.1. Nanoporous Hydrogel (NPHG)

Crosslinked thermosensitive hydrogels of poly(*n*-isopropylacrylamide) (cPNIPAM) nanoporous hydrogels were prepared by free radical polymerization of NIPAM (0.5 M) and 10 mM BIS as crosslinker agent, using APS (0.001 g/mL) and TEMED (10  $\mu\text{L}/\text{mL}$ ) as redox initiator and activator, respectively. The wet gel pieces were washed with running distilled water to remove any unreacted monomers and initiator.

#### 2.3.2. Macroporous Hydrogel (MPHG)

cPNIPAM macroporous cryogels were produced via free radical copolymerization of NIPAM (0.5 M) with AMPS (feed ratio 0.98:0.2). BIS was used as a crosslinker (2% in moles) and APS (1 mg/mL) was used as initiator. After addition of the initiators at 5 °C, the solutions were transferred into a glass syringe (1 mL) and sealed. Then, the syringe was placed into a polystyrene box and frozen at -18 °C, with the box open at the bottom. The reaction time was 24 h. After the polymerization finished, the

syringe was unfrozen at ambient 25 °C. The wet gel pieces were washed with running distilled water to remove any unreacted monomers and initiator.

#### 2.4. Synthesis of Conducting Polymer (Polyaniline and Polypyrrole) Nanoparticles

##### 2.4.1. Polyaniline Nanospheres (PANI-NS)

Polyaniline nanospheres (PANI-NS) were synthesized by precipitation polymerization from a solution of ANI-HCl (0.2 M) in water, using APS (0.25 M) as the oxidant in presence of a 2% w/w stabilizer (PVP) in water, as previously reported [35]. Polymerization was carried out at room temperature for 30 min and finally, a green dispersion of nanoparticles was obtained. The nanoparticles were purified by several centrifugation/redispersion cycles in water.

##### 2.4.2. Polyaniline Nanofibers (PANI-NF)

Polyaniline nanofibers (PANI-NF) were produced using the method reported before [36]. Briefly, the monomer (ANI, 24 mmol) was dissolved in 25 mL of an organic solvent (CHCl<sub>3</sub>) and APS (6 mmol) was dissolved 25 mL of HCl (1 M)/water. A liquid-liquid interface was generated, and polymerization of the monomer to obtain nanofibers occurred during 24 h in the dark. Finally, the aqueous phase containing the nano-objects was collected, and the nanofibers washed by several centrifugation/redispersion cycles in water.

##### 2.4.3. Polypyrrole Nanospheres (PPy-NS)

Polypyrrole spherical nanoparticles (PPy-NS) were obtained by a modification of the method described before [37]. The synthesis was carried out using APS (0.08 M) as an oxidant of the aqueous solution (0.043 M) of the monomer (Py). To stabilize the obtained nanoparticles, an aqueous solution of PVP (1% w/w) was used. The synthetic process was made in 30 min at 25 °C. The nanoparticles were purified by several centrifugation/redispersion cycles in water.

#### 2.5. Synthetic Methods of Composite Materials

The composite materials were made as 10 mm diameter discs, of 3 mm thickness. All measurements were made with the disks wet (no water excess) in air placed in a enclosed box (no air flux).

##### 2.5.1. In Situ Polymerization of Aniline or Pyrrole Inside a Nanoporous Hydrogel (PH)

Pieces of dry hydrogels were immersed into a solution with 0.1 M monomer (ANI or Py) in 1 M HCl, until all the solution was absorbed. A known amount of APS (equimolar to the monomer) was then added as oxidant to produce the conducting polymer inside the gel. The polymerization was carried out for 2 h at 25 °C. After the polymerization was finished, the nanocomposites were washed in stirring distilled water for 24 h.

##### 2.5.2. In Situ Formation of cPNIPAM around Conducting Polymer Nanoparticles (GAN)

Nanocomposites were synthesized by free radical polymerization of NIPAM with AMPS in a ratio 98:2 (molar), and BIS (2% molar ratio with the monomers) as crosslinker agent. Both monomers were dissolved in diluted dispersions (0.1 mg/mL) of each kind of nanoparticles. Then, polymerization initiators (APS and TEMED) were added (0.001 g/mL and 10 µL/mL, respectively) to obtain the nanocomposites after 30 min of reaction at 20 °C. After the polymerization process, nanocomposites were immersed in distilled water at room temperature for 48 h, renewing the water several times for remove unreacted chemicals.

### 2.5.3. Absorption of Conducting Polymers Nanoparticles into Macroporous Hydrogels (INH)

The macroporous hydrogels were dried in air and then swelled in dispersions of the conducting nanoparticles (1% p/v). The nanocomposites were washed with running distilled water.

### 2.5.4. Loading of Polyanilines from Solution into Nanoporous Hydrogels (AMH)

Dry cPNIPAM hydrogels were immersed in the different PANI solutions (PANI-EB in NMP (1% p/v)), PANI-ES (0.5% p/v) in  $\text{CHCl}_3$  and PANI-b-PNIPAM (0.1% p/v) in water. The original solvent was removed by heating under vacuum and then re-swollen in water with the appropriate pH.

## 2.6. Modulating the Doping State of the Conducting Polymer

### 2.6.1. By Protonation/Deprotonation

To set the protonation state, dry pieces of each nanocomposite samples were impregnated with acid or basic solution until they swelled to equilibrium, and left by 12 h in the solution. Then, the samples were wiped out with filter paper to remove the solution excess.

### 2.6.2. By Oxidation/Reduction

To reduce the conducting polymer inside the nanocomposite, dry pieces of each material (in the oxidized state) were impregnated with 0.1 M solution of phenylhydrazine/0.1 M  $\text{NH}_4\text{OH}$ , until they swelled to equilibrium, and left by 12 h in the solution. Then, the samples were wiped out with filter paper to remove the solution excess.

## 2.7. Electromagnetic Radiation Form Used as Input

### 2.7.1. Microwave Irradiation

The microwave irradiation of the nanocomposites was carried out with nanocomposite pieces placed in glass Petri dishes with lid. A beaker with 50 mL of distilled water was placed inside the oven to maintain 100% humidity. Optical photographs were taken with an electronic camera before and after exposition of the gels to microwaves, by extracting the samples from the oven and rapidly taking the photographs. The experiments were performed in a commercial multimode microwave oven (2.4 GHz, 700 W nominal power). The power setting can be 10, 20, 50, 80 and 100% of the nominal value. Such levels describe the number of pulses per second. The temperature system was measured with a thermographic camera (TESTO 868, Testo, Lenzkich, Germany).

### 2.7.2. Near Infrared (NIR I) Light Irradiation

NIR I light irradiation was made using a homemade irradiator, using a 3 W, 850 nm light emitting diode (LED). The LED irradiates from below the nanocomposite pieces placed on glass slides. The temperature was measured using a thermographic camera (TESTO 868) or an infrared thermometer (DeWALT<sup>®</sup>, DCT414S1, Baltimore, MD, USA).

### 2.7.3. Radiofrequency Irradiation

Small pieces of composite hydrogels (ca. 1.5 g) were placed into glass Petri dishes and irradiated using a RF generator (YNB Xiamen induction sealing device, Xiamen, China, 30 kHz, 1200 W). Experiments were conducted for 420 s, taking photographs at initial and final states. The temperature of each material was measured with an infrared thermometer (DeWALT<sup>®</sup>, DCT414S1).

### 2.7.4. Characterization

The size and distribution of nanoparticles was studied using Dynamic Light Scattering (DLS) in a commercial Malvern 4700 spectrometer (Malvern Instruments, Malvern, UK) equipped with a 488 nm

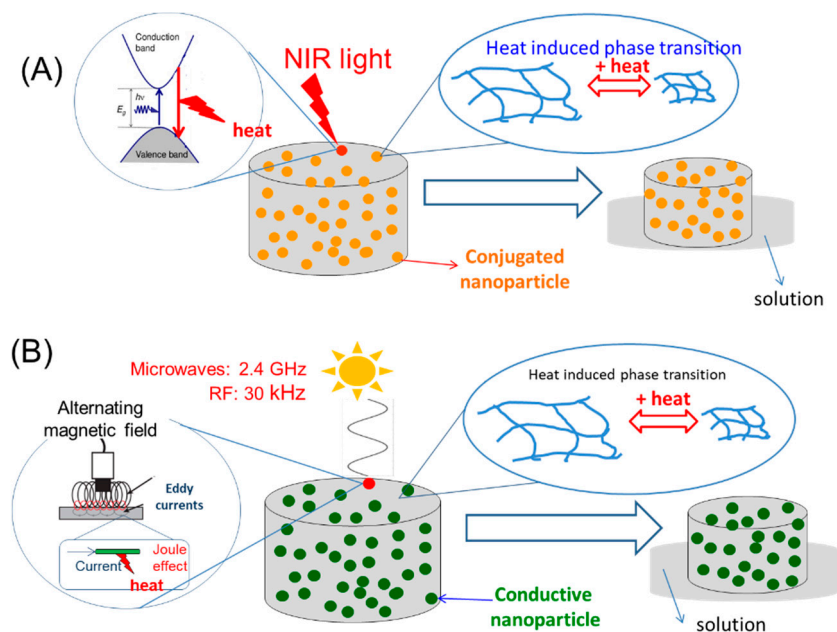


laser (OBIS). The topography of the hydrogel were determined in a Scanning Electron Microscope (SEM) Carl Zeiss EVO MA10 (Carl Zeiss, Oberkochen, Germany).

### 3. Results

#### 3.1. Product Property of the Nanocomposites

The goal of producing nanocomposites made of a dispersed conducting polymer phase inside a smart (thermosensitive) hydrogel matrix is to build materials with product properties (electromagnetic absorption X thermosensitive phase transition). The mechanism of coupling between both properties is described in Scheme 1.



**Scheme 1.** Mechanism of action underlying the effect of different forms of electromagnetic radiation on the thermomechanical materials: (A) near infrared (NIR) light input; and (B) Microwaves/RF (radiofrequency) input in electromagnetic radiation driven thermomechanical (ER-T-MCh) materials.

As can be seen, while all are electromagnetic radiation (ER), the NIR light and other ER induce heating in different ways. NIR light is absorbed in electronic transitions of conjugated polymers. The excited electron decays non radiatively releasing the energy to molecular vibrations that come out as heat. On the other hand, microwaves and radiofrequency are alternating magnetic fields which induce Eddy currents in the conducting polymer. The Eddy currents passing through the conducting polymer generates heat by Joule effect. While any conjugated polymer will produce heat when absorbs NIR light, only conducting polymers produce heat when ER (RF or microwaves) is applied.

The goal property of the nanocomposite is the ER driven thermomechanical (ER-T-MCh) effect which arises as the product of: electromagnetic radiation absorption (ERA) and heat induced phase transition (HIPT). Therefore:

$$ER-T-MCh = ERA \times HIPT \tag{1}$$

where X is the product operator. If ERA or HIPT are changed, ER-T-MCh is affected. If ERA or HIPT are either absent, ER-T-MCh is absent.

### 3.1.1. Electromagnetic Radiation Absorption (ERA)

The electromagnetic absorption is linked to the extended conjugation in the conducting polymer chains. However, it depends on the radiation used. The NIR photons cause electron transitions between molecular states or band structures in the polymer (Scheme 1A). Most conducting polymers, in the oxidized/doped states show absorption bands in NIR I wavelength range (700–850 nm). Therefore, light is absorbed, and the energy is converted into heat. The absorption in the NIR I is particularly useful, since biological tissue is relatively transparent in the NIR I [38]. NIR I light (e.g., 808 nm) can heat also PANI chains which are in the undoped and non-conductive state (emeraldine base) since the material has a finite absorption at that wavelength. However, if PANI redox state is changed, reducing emeraldine (doped and conductive) to leucoemeraldine (undoped and not conductive) only the UV absorption remains, and the polymer cannot be heated up by NIR I light. In this way, the HIPT of the nanocomposite can be modulated by the redox state. Such behavior is intrinsic to all conductive polymers. On the other hand, radiofrequency (30 kHz) and microwave (2.4 GHz) radiation heat up conducting PANI but should not heat the non-conducting PANI (emeraldine base). The heating mechanism (Scheme 1B) involves the generation of Eddy currents in the conductor [39], and the heating up by Joule effect [40]. Such mechanism only works for conductors and it can be switched off changing the conductivity of the polymer. This can be done by deprotonation (decrease by 3–4 orders of magnitude) or oxidation/reduction of PANI. In the case of other conductive polymers (e.g., PPy) the switching could be made only by oxidation/reduction since deprotonation only reduces the conductivity by an order of magnitude [41].

### 3.1.2. Heat-Induced Phase Transition (HIPT)

This is a well-known property of smart hydrogels (e.g., PNIPAM). The free polymer chains (between crosslinks) are extended in solution by interaction with the solvent. When the gel is heated, some groups increase its mobility, and the interactions with the solvent (e.g., hydrogen bonding) are broken. At the lower critical solution temperature (LCST), the polymer chains suffer a coil to globule transition where the chains lose interactions with the solvent and interactions are stronger between chain segments [42]. The solvent is expelled from the gel and the volume of the gel decreases because the size of the globules is smaller than the extended chains [43]. The fact that both the ER absorbing nanomaterial and the hydrogel are polymers that can be produced by soft chemistry allows different ways to produce the nanocomposites.

## 3.2. INH: Loading Preformed Conducting Polymer Nanoparticles Inside Macroporous Hydrogels

The simplest way to fabricate the nanocomposite, quite similar to the process of fabrication of fiber reinforced composite materials, involves the loading of nanoparticles by diffusion into the hydrogel. This can be done by swelling the dry hydrogel in a dispersion of the nanoparticles. (Scheme S1). The thermosensitive hydrogel is made by polymerization of an appropriate monomer (e.g., *N*-isopropylacrylamide, NIPAM) in a 3D matrix, using a divinyllic reactant as crosslinker. The amount of crosslinker is low (<5%). Therefore, the mean chain length between crosslinks is large and the gel is mainly made of linear chains. The material (e.g., crosslinked NIPAM or cPNIPAM) show strong swelling in water and related solvents. The nanoparticles size should be much smaller than the size of the pores to allow diffusion inside the hydrogel. Since PANI nanoparticles have a size as large as 200 nm [44], they cannot enter the pores of nanoporous hydrogels (pore diameter smaller than 50 nm). To overcome that, the gels should contain large macropores. To do that, ice crystals were used as the template by performing the polymerization at  $-20\text{ }^{\circ}\text{C}$ , in the frozen state [45]. Cryogelation has the advantage of producing pores with large aspect ratio, which can be used to transport nanoparticles inside the gel. In that way, not only nearly spherical nanoparticles but also PANI nanofibers (ca. 50 nm diameter and up to 10  $\mu\text{m}$  length) can be absorbed (Figure 1).





**Figure 1.** Photographs of poly(*N*-isopropylacrylamide) (PNIPAM) (with 2% 2-acrylamido-2-methyl-1-propanesulfonic acid (AMPS)) hydrogels after immersion in a dispersion of polyaniline (PANI) nanofibers. The nanoporous hydrogel (**left**) was made by polymerization at ambient temperature, where the macroporous hydrogel (**right**) was made by polymerization using cryogelation ( $-20\text{ }^{\circ}\text{C}$ ). Then, both were exposed to a dispersion (1% p/v) of PANI nanofibers in water. Both gels were exposed to 700 W of microwave radiation by 30 s.

The nanoparticles enter the pores, but are not released upon gel collapse. It seems that the nanoparticles are strongly adsorbed on the pore surface [46]. Accordingly, when gels without macropores (produced without cryogelation) are immersed in the dispersion, the nanoparticles do not enter the mass of the gel but are adsorbed irreversibly in the outer gel surface (Figure 1). Upon irradiation with microwaves, the nanocomposite collapse releasing the inner solution (Figure 1, right), while the hydrogel (Figure 1, left) remains unchanged. The microwave radiation (700 W, 2.4 GHz) interacts with the conducting nanofibers producing Eddy currents which circulate in the conducting nanofibers and produces heat by Joule effect (Scheme 1). The heat is transferred to the PNIPAM matrix, inducing the phase transition which is shown as volume collapse, with expulsion of the inner solution (Scheme 1). A similar effect is observed when radiofrequency (RF, 1000 W, 30 kHz) is used (Scheme 1). Additionally, irradiation with NIR I laser light (808 nm, 100 mW) also induces volume transition but due to optical absorption of NIR I photons (Scheme 1). Therefore, the nanocomposite produced by this method is an effective ER-T-MCh material. Since the macroporous hydrogel and the PANI nanoparticles can be characterized before combining, this is the most reproducible method to produce nanocomposites. On the other hand, since the macropores are millimeter long, only macroscopic pieces of gel can be built. The macroporous hydrogels are mechanically weak due to the large void volume but such properties can be improved by filling the macropores with more hydrogel after the nanoparticles are loaded.

### 3.3. GAN: *In Situ* Polymerization of the Smart Hydrogel Matrix around the Dispersion of Conductive Polymer Nanoparticles

Another method involves the formation of the smart hydrogel matrix around conducting polymer nanoparticles, which should be evenly dispersed in the polymerization solution (Scheme S2). Stable dispersions of conducting polymer nanoparticles can be made by different methods. The nanoparticles are thoroughly characterized using scanning electron microscopy, transmission electron microscopy and dynamic light scattering. The full characterization of the nanoparticles is an advantage of this method compared to the others presented in this work. The gel is made by the usual radical polymerization with a crosslinker. It was found that using the same amount of cross-linker than in the absence of nanoparticles, mechanically weak films or even a viscous solution are obtained. It seems that the growing radical chains react with the conjugated polymer surface of the nanoparticles, inhibiting the growth of the polymer chains. Therefore, the concentration of hydrogel reactants was doubled to obtain mechanically stable hydrogels. Another problem with this approach is that the gelification process could induce the aggregation of the nanoparticles due to excluded volume effects. It seems that some aggregation occurs in the case of cPNIPAM formation around PVP stabilized PANI particles.

Applying radiofrequency to this kind of nanocomposite, the temperature increased (Figure 2) more than the underlying aqueous solutions.

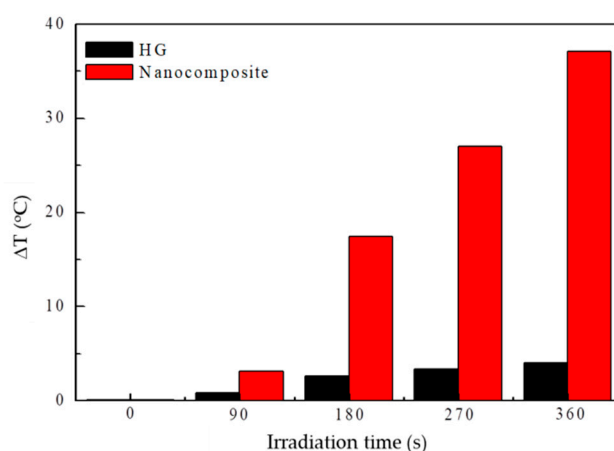


**Figure 2.** Effect of RF (30 kHz, 1000 W) irradiation on the hydrogel matrix (HG, black bars) and the nanocomposite (red bars) produced by formation of Crosslinked thermosensitive hydrogels of poly(*n*-isopropylacrylamide) (cPNIPAM) around PANI nanoparticles (stabilized with polyvinylpyrrolidone (PVP)). The temperature was measured with a thermographic camera.

Similar materials are made by gelation of cPNIPAM around PANI nanofibers or polypyrrole (PPy) nanospheres. The ER-T-MCh behavior of those materials is quite similar to the one described above [47]. The nanocomposites formed in this way show ER-T-MCh behavior to be induced by RF and microwaves, but not by NIR light [47]. It seems that the aggregates scatter the NIR light not allowing light to reach PANI nanoparticles and heat the composite. The method seems to be the less useful for producing ER-T-MCh nanocomposites using PANI or PPy nanoparticles.

### 3.4. PIH: *In Situ* Polymerization of the Conductive Polymer Inside the Smart Hydrogel Matrix

#### 3.4.1. Semi-Interpenetrated Network or Nanocomposite?

The most widely used way to produce the nanocomposite involves swelling the hydrogel in a solution of a conducting polymer monomer (e.g., aniline) followed by the diffusion of the oxidant (e.g., APS), allowing synthesizing the conducting polymer inside the hydrogel matrix [48], (Scheme S3). The order of incorporation of the reactants is relevant, as large ratios of oxidant/monomer lead to polymer degradation. Since a linear conducting polymer is produced inside a crosslinked network, the resulting material was considered [49], to be a semi-interpenetrated network (sIPN of PANI in cPNIPAM), that is a polymer blend. However, we have shown data suggesting that nanodomains of PANI are present filling of the pores of the hydrogel [50]. This is reasonable since the conducting polymer is insoluble in water and the polymerization in solution occurs with precipitation. The presence of the conducting polymer does not affect the LCST of the hydrogel chains as expected if a strong interaction exists. Such effect is observed when NIPAM is copolymerized with other co-monomers [51], but not when other acrylamides are synthesized inside cPNIPAM [52], suggesting that phase segregation is a general behavior. On the other hand, it has been reported that polymerization of aniline or pyrrole inside cPNIPAM in the presence of phytic acid produces interpenetrated networks [53]. Since it is known that polymerization of aniline in the presence of phytic acid produces a conductive polymer gel [54], an interpenetrated network (IPN) could be formed between PANI gel (crosslinked by phytic acid) and cPNIPAM gel. No LCST measurement was reported [54], but it has been shown that the gel is thermally switched at 50 °C (higher than the LCST of PNIPAM of 32–33 °C), suggesting interaction between both networks as shown above.

### 3.4.2. “Smart” Behavior: Effect of Electromagnetic Irradiation (microwaves) on the Conductive Nanocomposites

Having produced a nanocomposite by in situ polymerization inside the hydrogel (IPH), we studied the effect of microwaves compared to the hydrogel matrix under the same conditions. In Figure 3, a comparison of the effect of microwaves on the hydrogel (left piece in each panel) and the nanocomposite (right piece in each panel) is shown. It can be seen that both materials show a temperature (22 °C), slightly below the background, likely due to water evaporation from the wet materials. After applying 5 s of microwave irradiation (2.4 GHz, 70 W), the whole wet substrate, and the hydrogel piece heat up slightly (ca. 29 °C) due to microwave absorption by water. On the other hand, the nanocomposite heats up to 37 °C, which is likely due to the generation of Eddy currents in the conductor and the rise of the Joule effect. Since the nanocomposite temperature become higher than the LCST, the hydrogel matrix suffer a phase transition (coil to globule) of the free chains between crosslinks and the volume of the piece collapses, expelling the inner solution (Figure 3d). Gravimetric measurements of the hydrogel and nanocomposite pieces, before and after irradiation, confirm that the inner solution is expelled upon microwave irradiation of the nanocomposite while the hydrogel remains unaffected. The volume collapse is reversible (Figure S1). The size changes and the inner solution is expelled upon ER input (microwaves). After cooling, the size of the sample recovers its original value and no change in shape is observed.

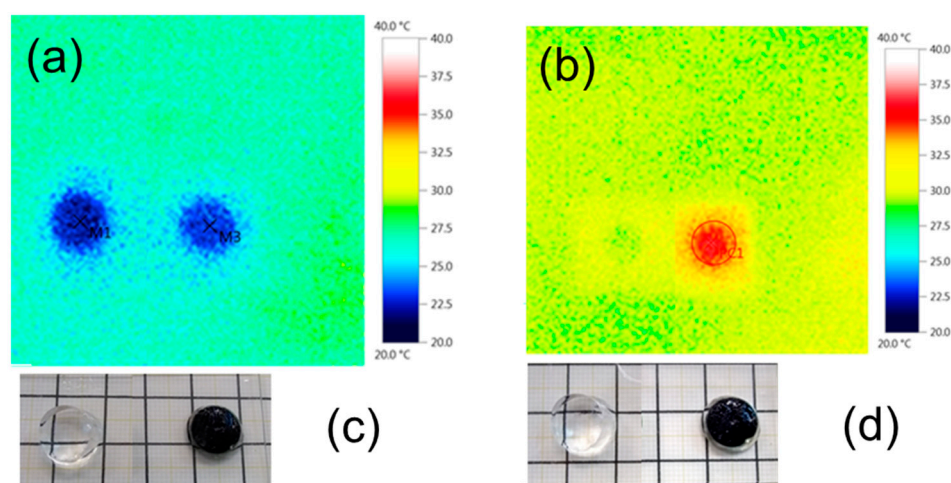


**Figure 3.** Effect of microwaves on the hydrogel and doped (protonated) nanocomposite. Above: thermographic images taken before (a) and after (b) application of 5 s of microwave irradiation. The scales at the left of each panel link color with temperatures. Below: optical images taken before (c) and after (d) application of 5 s of microwave irradiation. The transparent sample (left in (c,d)) correspond to the hydrogel matrix while the green sample (right in (c,d)) corresponds to the nanocomposite made by IPH.

### 3.4.3. Effect of Electromagnetic Irradiation (Microwaves) on the Non-Conductive (Deprotonated) Nanocomposite

In Figure 4 a comparison of the effect of microwave irradiation on the hydrogel (left piece in each panel) and the non-conductive (deprotonated) nanocomposite (right piece in each panel) is shown. Both materials were immersed in 0.1 M  $\text{NH}_4\text{OH}$  (2 h) to deprotonate the PANI nanodomains. As can be seen, the gels change from green (Figure 3) to blue. This is the expected spectral change between the emeraldine salt form (green) and emeraldine base form (blue) of PANI. The conductance of the piece was reduced by ca. 3 orders of magnitude. It can be seen that both materials show a temperature (23 °C), slightly below the background, likely due to water evaporation. After 5 s of microwave irradiation (2.4 GHz, 70 W), no effect was observed. However, after 10 s of microwave irradiation, the whole wet substrate, and the hydrogel piece heat up slightly (ca. 29 °C) due to absorption in water.

The nanocomposite (blue disks) is not heated up, nor collapses. Since the deprotonated (undoped) PANI is non-conductive, no Eddy currents are generated, and there is no additional heat generated by Joule effect. Since the nanocomposite temperature remains lower than the LCST, the nanocomposite volume stays unaltered (Figure 4d).

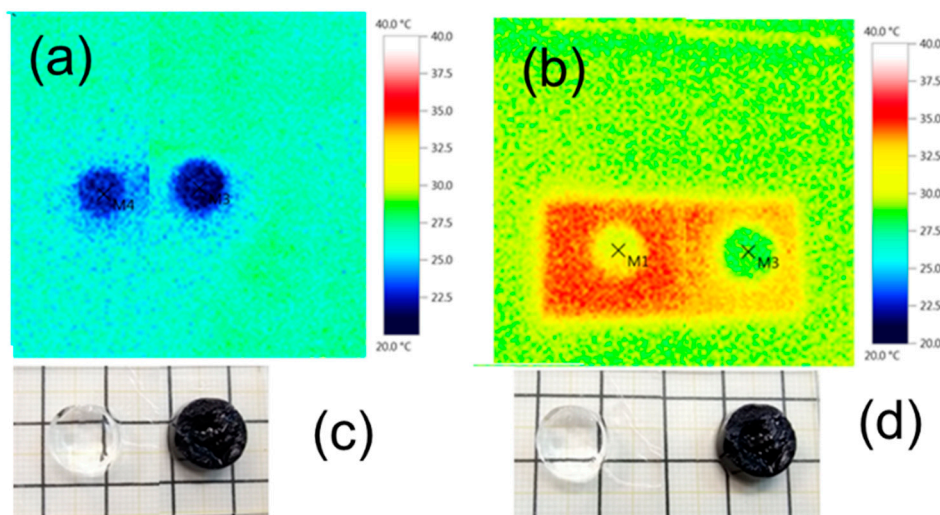


**Figure 4.** Effect of microwaves on the hydrogel (transparent) and the deprotonated (undoped) nanocomposite (blue) made by IPH. The upper panels (a,b) show the thermographic images before (a) and after (b) irradiation with microwaves by 10 s. The scales at the left of each panel link color with temperatures. The lower panels (c,d) show the optical photographs of the hydrogel (transparent, left) and nanocomposite (blue, right) before (c) and after (d) microwave (2.4 GHz, 70 W) irradiation for 10 s.

The observed effect allows producing smart materials (sER-T-MCh) since the observed response depends on the surrounding media. As it is, the material could be used in diagnostics as the pH of an inner tissue could be sensed by applying microwaves to a nanocomposite probe and reading out the probe size using an imaging technique. The smart property of reacting to pH is exclusive of PANI since tests with nanocomposites with polypyrrole (made by IPH) does not show effect of pH. This is related to the fact that polypyrrole conductivity changes by deprotonation but only by a factor of 5 [41]. Lower sensitivity to the surroundings (e.g., biological media) could be an advantage if only the ER-T-MCh property is of interest. This can be done easily choosing the conducting polymer to load in the nanocomposite. On the other hand, the nanocomposite containing deprotonated heats up and suffer phase transition upon illumination with NIR light. Since deprotonated PANI is not conductive, it is inactive upon irradiation with microwaves or RF. However, deprotonated PANI still absorbs NIR light because it has extended conjugation.

#### 3.4.4. Effect of Electromagnetic Irradiation (Microwaves) on the Non-Conductive (Reduced) Nanocomposite

Another way to change the conductivity of PANI implies the reduction of the emeraldine chains. In Figure 5, a comparison of the hydrogel (left piece in each panel) and the reduced nanocomposite (right piece in each panel) is shown. The hydrogel and the nanocomposite piece were immersed in phenylhydrazine solution (0.1 M, 12 h) and the green color changes to yellow-brown. The conductance of the piece decreases by two orders of magnitude. The quinonimine rings in the PANI chains are transformed from the emeraldine form (50% oxidation) to leucoemeraldine forms (0% oxidation). Since the species is unstable in air due to oxygen oxidation, a small concentration of the reductant is maintained in both samples.



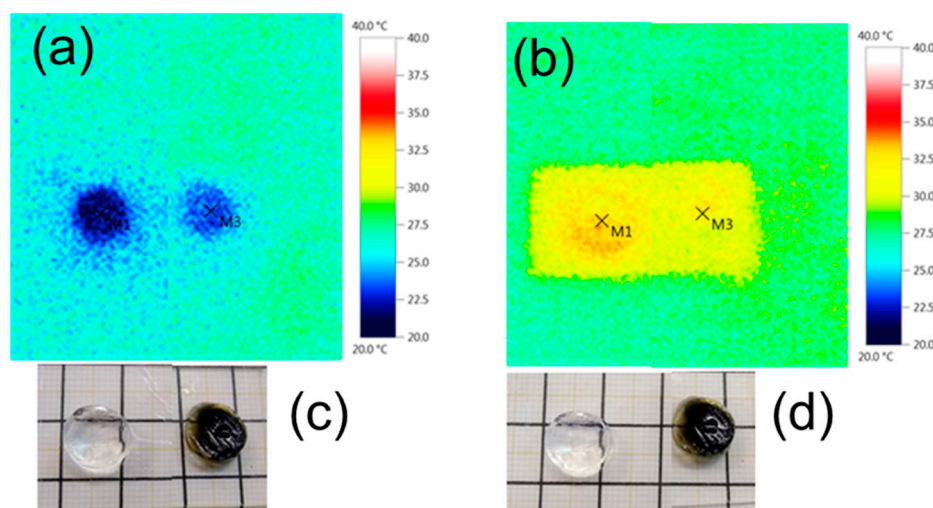
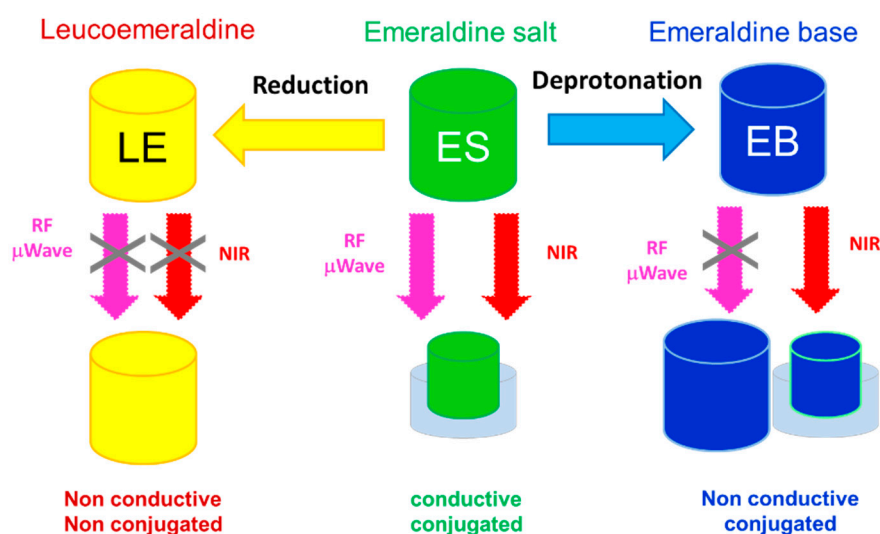


**Figure 5.** Comparative images of the hydrogel (transparent, left) and reduced (non-conductive) electromagnetic radiation thermomechanicochemical (ER-T-MCh) nanocomposite (brown, right) made by in situ polymerization of aniline loaded inside a cPNIPAM hydrogel (IPH). Before measurement, both samples were treated with a reductant (phenylhydrazine). The thermographic images are shown in the upper panels (a,b). The scales at the left of each panel link color with temperatures. The optical photographs are shown in the lower panels (c,d). The images in (a,c) show the samples before irradiation, while the images in (b,d) depict the materials after microwave irradiation (2.4 GHz, 70 W, 10 s).

It can be seen that both materials show a temperature (23 °C) that is slightly below the background, likely due to water evaporation. After 5 s of microwave irradiation (2.4 GHz, 70 W), no effect was observed. After 10 s, the whole wet substrate, and the hydrogel piece heat up slightly (ca. 29 °C) due to absorption of microwaves in water. The nanocomposite (brown disks) is not heated up; therefore, the phase transition does not occur and the volume does not decrease. It seems that reduced (undoped) PANI nanodomains are non-conductive and no Eddy currents are generated upon microwave irradiation. Therefore, no heat is produced by Joule effect. Since the nanocomposite temperature remains lower than the LCST, the volume of both pieces (hydrogel and nanocomposite) remains the same (Figure 5d). In the case of the reduced nanocomposite, illumination with NIR light does not lead to volume collapse. This is reasonable since the leucoemeraldine form of PANI does not have absorption in the NIR range; unlike the emeraldine salt or base forms [55], because it contains aniline moieties but no extended conjugation. This effect of the media on the ER-T-MCh property is not exclusive of PANI as the conductivity of any conducting polymer decreases sharply by reduction. Indeed, nanocomposite made by IPH of pyrrole showed the same effect. While obviously the reduction potential of the media used here is quite high, biological media also contain redox active biomolecules (e.g., ascorbic acid) which are able to reduce PANI.

The mechanism of “smart” changes in the sensitivity of PANI in NIPAM nanocomposite to different forms of electromagnetic radiation, upon deprotonation or reduction of the PANI component, is described in Scheme 2.





**Scheme 2.** Mechanism of the “smart” effect of deprotonation/reduction on the activity toward electromagnetic radiation of the nanocomposite made of PANI in cPNIPAM (IPH).

### 3.5. AMH: Loading Conducting Macromolecules inside the Smart Hydrogel Matrix

cPNIPAM strongly swells in water. Therefore, a soluble conducting polymer (CP) in water could be loaded inside the gel by swelling it in a solution of the CP. Accordingly; sulfonated polyaniline was loaded into polyacrylamide [56]. However, it was found that the soluble CP is released from the gel in basic solution. Doped PANI is only soluble in a few solvents, such as formic and sulfuric acid, while undoped PANI is soluble in *N*-methylpyrrolidone (NMP). It was found that cPNIPAM can be swelled in different common solvents (including NMP) [57]. Therefore, swelling a cPNIPAM piece in a PANI solution in NMP enables loading the linear PANI chains inside the hydrogel (Scheme S4). The phase transition temperature (LCST) of the hydrogel can be tuned by random copolymerization of the thermosensitive unit (e.g., NIPAM) with vinyl monomers (e.g., acrylic acid) bearing hydrophilic or hydrophobic groups. The incorporation of a hydrophilic group increases the LCST, while a hydrophobic group decreases the LCST [58]. Since conducting polymer chains are hydrophilic polyelectrolytes, the fixed charges and/or the counterions should increase the LCST of the hydrogel if present in the same phase. Accordingly, the LCST of the sIPN of PANI in cPNIPAM is of ca. 42 °C (while that of cPNIPAM is 32–34 °C) [59]. Therefore, the material is not a nanocomposite with two separate phases, but an intimate polymer blend with only one phase. Since the material contains a conducting polymer, it can be heated up by illumination with NIR I light, irradiation with microwaves or radiofrequency (Figure 6). Additionally, it can be seen that the gel collapses when a temperature is reached that is higher than the LCST of the nanocomposite (insert in Figure 6).

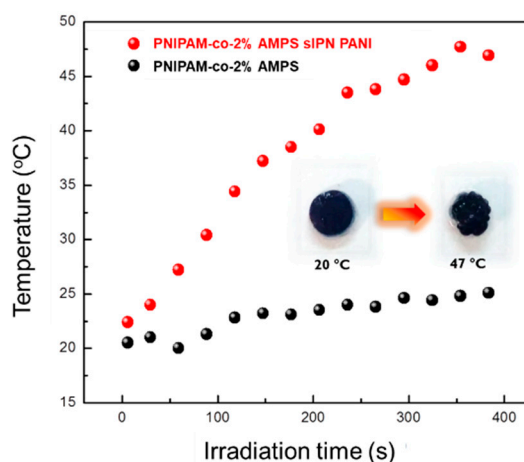


**Figure 6.** Measurements of temperature (red spheres) of a material (sIPN of PANI in PNIPAM-co-2% AMPS made by AMH) subjected to RF (1000 W, 30 kHz) irradiation. For comparison, the temperature of the hydrogel matrix (black spheres) during irradiation is shown. The temperature was measured using a thermographic camera. In the insert, the optical photographs of the ER-T-MCh material before (20 °C) and after 400 s of irradiation (47 °C) are shown.

The change of LCST due to the interaction between the conducting polymer and the thermosensitive polymer chains is a disadvantage of this fabrication method, since it makes it difficult to predict the phase transition temperature of the final material. To use this method, it is necessary to have the conducting polymer soluble in a solvent able to swell the hydrogel. It is known that PANI can be solubilized in common solvents (e.g.,  $\text{CHCl}_3$ ), which swell cPNIPAM [57], by doping with amphiphilic counterions [60]. Therefore, cPNIPAM gels were swollen in solutions of PANI (emeraldine salt with camphorsulfonate as amphiphilic counterion) in  $\text{CHCl}_3$  [61,62]. The nanocomposite is then dried by evaporation of the solvent, and swollen in water. Upon application of microwave radiation, the gel heats up and collapse suggesting that the P-T-MCh property is present. Recently, we showed that it was possible to synthesize a block copolymer of NIPAM and aniline (PNIPAM-*b*-PANI) by telechelic polymerization using 4-aminothiophenol as coupling agent [34]. The copolymer is soluble in water and can be loaded inside cPNIPAM by swelling the gel in a PNIPAM-*b*-PANI solution. Preliminary results suggest that it is possible to collapse the gel by irradiation with microwaves or NIR I light. Moreover, the LCST also increases due to interaction of the PNIPAM chains with the PANI chains, suggesting that a semi-interpenetrated PANI in cPNIPAM was formed. The increase of LCST due to the interaction between the ER absorbing (PANI) and thermosensitive (PNIPAM) chains is a disadvantage since could depend on the amount of PANI and/or the chemical nature of the conductive polymer. It could be interesting to use the method with polypyrrole (PPy), which is more hydrophobic than PANI (LCST should decrease) but no solvent is known for unmodified PPy. Since the LCST of sIPN PANI in PNIPAM is higher, (42 °C) that of PNIPAM or the nanocomposites (32–33 °C), more energy has to be applied to reach the LCST. Therefore, a quantitative difference exists for samples of the same size and PANI content.

### 3.6. Comparison between Composite Materials Made Using Different Synthetic Methods

The result of the application of different forms of electromagnetic radiation on the composite materials made by different synthetic methods is summarized in Table 1.

**Table 1.** Comparative effect of different forms of electromagnetic radiation (ER) on the composite materials produced by different synthetic methods.

Synthetic Method	State of Polyaniline (PANI)	Electromagnetic Radiation		
		Near Infrared Light (NIR I) (3 W, 850 nm)	Microwaves (70 W, 2.4 GHz)	Radiofrequency (RF) (1000 W, 30 kHz)
INH *	Protonated	ON	ON	ON
GAN #	Protonated	OFF	ON	ON
PIH *	Protonated	ON	ON	ON
PIH *	Deprotonated	ON	OFF	OFF
PIH *	Reduced	OFF	OFF	OFF
AMH *	Protonated	ON	ON	ON

\* Lower critical solution temperature (LCST) = 33 °C, # LCST = 42 °C.

In Table 1, ON indicates that a visible volume collapse (and temperatures reaching above LCST) is achieved by a given time (see text), where the same radiation applied in the hydrogel matrix does not show an effect. OFF indicates that no noticeable difference is observed with the hydrogel matrix. In all cases, the material was tested with the PANI component in the protonated state (emeraldine salt (ES) = conductive and conjugated). Additionally, in the case of the nanocomposite made by PIH, the materials were also tested with PANI in the deprotonated (emeraldine base (EB) = non-conductive but conjugated) and reduced (leucoemeraldine (LE) = non-conductive and non-conjugated) (see Scheme 2). As can be seen, using any of the four synthetic methods produces materials active as ER-T-MCh, except for the nanocomposite made by GAN when NIR light is used. It is likely that nanoparticle aggregation produces a large amount of light scattering, which does not allow the light to reach the PANI nanoparticles.

On the other hand, in the case of the material made by PIH, the nanocomposite is active in the protonated (ES) and deprotonated (EB) state when NIR is used as input but only the ES state is active when microwaves or RF are used as input. Moreover, the nanocomposite is inactive for any form of electromagnetic radiation when the PANI is reduced (LE). This data agrees with the mechanism described in Schemes 1 and 2. Conductive materials (PANI ES) heat up by application of microwaves or RF due to the generation of Eddy currents which gives rise to Joule effect. On the other hand, NIR light is absorbed in conjugated materials (PANI ES and EB) and heats up the nanocomposite. Reduced PANI (LE) is neither conductive nor conjugated, and could not be heated up by any of the electromagnetic radiation applied. It should be mentioned that all the forms of radiation used has a background absorption in the hydrogel matrix. Therefore, we detect a differential effect between the composite and its matrix.

#### 4. Discussion

The results described allow the establishment of thermomechanicochemical nanocomposites driven by electromagnetic radiation (ER-T-MCh) materials as a new class of nanocomposites with product properties. Specifically, conducting polymers dispersed in thermosensitive hydrogels show clear ER-T-MCh activity. Moreover, the material reacts to external stimuli (pH, redox potential) with modulated ER-T-MCh effect. In this way, the material becomes a smart ER-T-MCh nanocomposite.

Three methods for producing nanocomposites are described: INH: absorption of conducting polymer nanoparticles inside porous thermosensitive hydrogels; GAN: trapping of conducting nanoparticles inside an in situ formed thermosensitive hydrogel matrix; and PIH: in situ polymerization of a conducting polymer inside the pores of a thermosensitive hydrogel matrix. Finally, a method (AMH) for the formation of macromolecular blends (semi-interpenetrated network) by absorbing conducting polymer molecules inside a nanoporous thermosensitive hydrogel is shown to produce an ER-T-MCh material. The advantages and disadvantages of the different methods are described in Table 2.

**Table 2.** Advantages and disadvantages of the different synthetic methods described before.

Synthetic Method	Advantages	Disadvantages
INH	<ul style="list-style-type: none"> <li>— independent characterization of the nanomaterial, <sup>1</sup> and hydrogel matrix. <sup>2</sup></li> <li>— free selection of the nanomaterials allowing simple screening of nanomaterial/hydrogel combinations.</li> <li>— physical synthesis with high reproducibility compared to chemical in situ synthesis where the presence of the other component could affect the reaction.</li> <li>— works with preformed nanomaterials.</li> </ul>	<ul style="list-style-type: none"> <li>— only macroscopic (&gt;1 mm) sized shapes due to macroporosity. <sup>3</sup></li> <li>— poor mechanical properties due to large porosity.</li> <li>— possible leakage of the nanomaterial upon solution expulsion (weak adsorption).</li> </ul>
GAN	<ul style="list-style-type: none"> <li>— simple synthesis</li> <li>— works with preformed nanomaterials.</li> <li>— good characterization of the nanomaterial. <sup>3</sup></li> </ul>	<ul style="list-style-type: none"> <li>— aggregation of the nanomaterial</li> <li>— inhibition of polymer growth/gelation by the nanomaterials.</li> <li>— poor characterization of the hydrogel. <sup>4</sup></li> <li>— poor reproducibility due to effects of the nanomaterial on the in situ gelation.</li> </ul>
PIH	<ul style="list-style-type: none"> <li>— simple synthesis</li> <li>— any size of the pieces (including nanometric)</li> <li>— good characterization of the hydrogel matrix. <sup>2</sup></li> </ul>	<ul style="list-style-type: none"> <li>— requires the reactants to produce the nanomaterial to be soluble in the solvent that swells the gel.</li> <li>— poor characterization of the nanomaterial. <sup>5</sup></li> <li>— poor reproducibility due to effects of the hydrogel on the formation of nanoparticles.</li> </ul>
AMH	<ul style="list-style-type: none"> <li>— produces a true semi-interpenetrated network</li> <li>— any size of the pieces (including nanometric)</li> <li>— physical synthesis of the composite with high reproducibility.</li> </ul>	<ul style="list-style-type: none"> <li>— requires the loaded polymer to be soluble in the solvent that swells the gel.</li> <li>— polymer could be released from the material upon volume collapse.</li> <li>— the LCST is affected by interaction of the loaded polymer with the thermosensitive chains in the hydrogel matrix.</li> </ul>

<sup>1</sup> The pre-formed nanomaterial can be fully characterized with DLS, SEM and transmission electron microscopy (TEM). <sup>2</sup> The pre-formed hydrogel can be fully characterized: swelling kinetics, mechanical properties, open porosity, LCST determination and release kinetics. <sup>3</sup> This disadvantage can be overcome using small (<20 nm) conducting polymer nanoparticles and porous hydrogels with large mesopores or small macropores (40 < d < 100 nm). <sup>4</sup> In situ gelation makes that the hydrogel matrix could not be independently characterized. <sup>5</sup> In situ formation of the nanomaterial leaves the nanomaterial poorly characterized.

The different materials show mechanochemical changes (volume/density, solution release, hydrophobicity, mechanical properties, opacity, etc.) upon input of electromagnetic radiation (NIR I light, microwaves, and radiofrequency). The synthetic method has almost (with NIR I input with GAN being the exception) no effect on the ER-T-MCh property of the nanocomposite. On the other hand, it has a clear effect on the possibility of building different sized structures. Fabrication of nanostructures with INH is impossible and with GAN involves a redesign of the method while ER-T-MCh of nanometric size is easily made by PIH [63], or AMH. The INH method involves the physical mixing of two well characterized materials: conducting polymer nanoparticles and a macroporous thermosensitive hydrogel. Besides the photothermal effect, the interaction between the materials is minimal. Therefore, the mechanical properties depend mainly on those of the hydrogel matrix which can be set in advance.

If the component material (dispersed nanomaterial or hydrogel matrix) could be pre-formed in its final form and then physically integrated with the other component, it could be fully characterized before compositing. Therefore, in the case of INH, both the nanoparticle and the hydrogel could be characterized before compositing making it the best characterized material. The materials produced by GAN are similar but the strong effect of the NPs on the gelation and the aggregation of the NP during synthesis makes this method the less reproducible and less useful. In situ formation either of the nanomaterial (PIH) or the hydrogel (GAN) leaves one component poorly characterized. It should be noted that both components are carbon-based. Therefore, electronic techniques (SEM, TEM) show little contrast between the phases unlikely when an inorganic (e.g., gold nanoparticles) material is dispersed in a polymeric hydrogel. The deswelling process is reversible and can be repeated several times without noticeable damage. The mechanical properties of the hydrogels used as matrices and the nanocomposites have been studied previously [46,47,50,57,59,61,64], in the swollen (uncollapsed state). In general, the gels are soft materials with elastic modulus below 10 kPa [64]. The incorporation of the nanomaterial somewhat increase the modulus due to a decrease in the plasticity by the dispersed phase. However, other strategies, like double networking [65] or crosslinking with nanoparticles [31], should give better mechanical properties. In an actual application (e.g., triggered drug release), several parameters have to be taken into account like background absorption/scattering, heat dissipation, sample size, etc., to design real devices. On the other hand, this is the main method of nanocomposite synthesis when the formation of the nanomaterial (e.g., carbon nanotubes) is not compatible with the presence of the gel.

**Supplementary Materials:** The following are available online at <http://www.mdpi.com/2504-477X/4/1/3/s1>, Figure S1: Effect of microwaves on the doped (protonated) nanocomposite (made by PIH) along the heating and cooling cycle. Photographs: (a) Before irradiation ( $T = 29.7\text{ }^{\circ}\text{C}$ ), (b) After microwave irradiation (30 s, 70 W) ( $T = 38.9\text{ }^{\circ}\text{C}$ ), (c) After cooling in air ( $T = 27.3\text{ }^{\circ}\text{C}$ ). Temperatures measured using a thermographic camera; Scheme S1: Formation of the nanocomposite by loading nanoparticles inside macroporous hydrogels (INH); Scheme S2: In-situ gelation of the smart hydrogel matrix around the dispersion of conductive polymer nanoparticles (GAN); Scheme S3: In-situ polymerization of the conductive polymer inside the smart hydrogel matrix to produce a nanocomposite (IPH); Scheme S4: PANI chains loading from solution into cPNIPAM hydrogel (AMH).

**Author Contributions:** Conceptualization, M.A.M. and C.A.B.; methodology, C.A.B., M.A.M., S.B.A., D.F.A.; investigation, K.R., S.B.A., R.G., M.V.M., R.R., and E.A.C.; resources, C.A.B., D.F.A.; data curation, C.R.R., D.F.A.; writing—original draft preparation, C.A.B.; writing—review and editing, C.A.B. and M.A.M.; supervision, C.A.B., M.A.M.; project administration, C.A.B., D.F.A.; funding acquisition, C.R.R., D.F.A. All authors have read and agreed to the published version of the manuscript.

**Funding:** This research was funded by FONCYT, grant number PICT 1760/2016 and PDTS-CIN-CONICET IP 436.

**Conflicts of Interest:** The authors declare no conflict of interest. The funders had no role in the design of the study; in the collection, analyses, or interpretation of data; in the writing of the manuscript, or in the decision to publish the results.

## References

1. Barbero, E.J. *Introduction to Composite Materials Design*; CRC Press: Boca Raton, FL, USA, 2017.
2. Hameed, N.; Kurian, T.; Yu, Y.; Parameswaranpillai, J. *Nanocomposite Materials: Synthesis, Properties and Applications*; CRC Press: Boca Raton, FL, USA, 2016.



3. Barbero, E.J. (Ed.) *Multifunctional Composites*; CreateSpace Independent Publishing Platform: Scottsdale Valley, CA, USA, 2015.
4. Gurses, A. *Introduction to Polymer-Clay Nanocomposites*; Jenny Stanford Publishing: Singapore, 2015.
5. Van Suchtelen, J. Product properties: A new application of composite materials. *Philips Res. Rep.* **1972**, *27*, 28–37.
6. Wu, C.; Zhou, S. Volume Phase Transition of Swollen Gels: Discontinuous or Continuous? *Macromolecules* **1997**, *30*, 574–576. [[CrossRef](#)]
7. Bischofberger, I.; Calzolari, D.C.E.; De Los Rios, P.; Jelezarov, I.; Trappe, V. Hydrophobic hydration of poly-N-isopropyl acrylamide: A matter of the mean energetic state of water. *Sci. Rep.* **2014**, *4*, 4377. [[CrossRef](#)] [[PubMed](#)]
8. Umapathi, R.; Reddy, P.M.; Rani, A.; Venkatesu, P. Influence of additives on thermoresponsive polymers in aqueous media: A case study of poly (N-isopropylacrylamide). *Phys. Chem. Chem. Phys.* **2018**, *20*, 9717–9744. [[CrossRef](#)]
9. Wang, Y.; Dong, M.; Guo, M.; Wang, X.; Zhou, J.; Lei, J.; Guo, C.; Qin, C. Agar/gelatin bilayer gel matrix fabricated by simple thermo-responsive sol-gel transition method. *Mat. Sci. Eng. C Mater.* **2017**, *77*, 293–299. [[CrossRef](#)]
10. Chen, H.; Shao, L.; Li, Q.; Wang, J. Gold nanorods and their plasmonic properties. *Chem. Soc. Rev.* **2013**, *42*, 2679–2724. [[CrossRef](#)]
11. Zhao, Y. A near-infrared light-responsive hybrid hydrogel based on UCST triblock copolymer and gold nanorods. *Polymers* **2017**, *9*, 238. [[CrossRef](#)]
12. Nehl, C.L.; Grady, N.K.; Goodrich, G.P.; Tam, F.; Halas, N.J.; Hafner, J.H. Scattering Spectra of Single Gold Nanoshells. *Nano Lett.* **2004**, *4*, 122355–122359. [[CrossRef](#)]
13. Messersmith, R.E.; Nusz, G.J.; Reed, S.M. Using the localized surface plasmon resonance of gold nanoparticles to monitor lipid membrane assembly and protein binding. *J. Phys. Chem. C* **2013**, *117*, 26725–26733. [[CrossRef](#)]
14. Sun, Z.; Yamauchi, Y.; Araoka, F.; Kim, Y.S.; Bergueiro, J.; Ishida, Y.; Ebina, Y.; Sasaki, T.; Hikima, T.; Aida, T. An Anisotropic Hydrogel Actuator Enabling Earthworm-Like Directed Peristaltic Crawling. *Angew. Chem.* **2018**, *57*, 15772–15776. [[CrossRef](#)]
15. Wu, Z.; Lin, X.; Zou, X.; Sun, J.; He, Q. Biodegradable protein-based rockets for drug transportation and light-triggered release. *ACS Appl. Mater. Interfaces* **2015**, *7*, 250–255. [[CrossRef](#)] [[PubMed](#)]
16. Gonçalves, R.; Larrea, A.; Sebastian, M.S.; Sebastian, V.; Martins, P.; Lanceros-Mendez, S. Synthesis and size dependent magnetostrictive response of ferrite nanoparticles and their application in magnetoelectric polymer-based multiferroic sensors. *J. Mater. Chem. C* **2016**, *4*, 10701–10706. [[CrossRef](#)]
17. Lee, E.; Kim, D.; Kim, H.; Yoon, J. Photothermally driven fast responding photo-actuators fabricated with comb-type hydrogels and magnetite nanoparticles. *Sci. Rep.* **2015**, *5*, 15124. [[CrossRef](#)] [[PubMed](#)]
18. Hou, K.; Wu, W.; Xia, M.; Zhu, M. A novel NIR laser switched nanocomposite hydrogel as remote stimuli smart valve. *Macromol. Mater. Eng.* **2017**, *302*, 1700213. [[CrossRef](#)]
19. Huang, H.; Kajiura, H.; Maruyama, R.; Kadono, K.; Noda, K. Relative optical absorption of metallic and semiconducting single-walled carbon nanotubes. *J. Phys. Chem. B* **2006**, *110*, 4686–4690. [[CrossRef](#)] [[PubMed](#)]
20. Zhang, H.; Zhu, X.; Ji, Y.; Jiao, X.; Chen, Q.; Hou, L.; Zhang, H.; Zhang, Z. Near-infrared-triggered in situ hybrid hydrogel system for synergistic cancer therapy. *J. Mater. Chem. B* **2015**, *3*, 6310–6326. [[CrossRef](#)]
21. Kim, D.; Lee, E.; Lee, H.S.; Yoon, J. Energy efficient glazing for adaptive solar control fabricated with photothermotropic hydrogels containing graphene oxide. *Sci. Rep.* **2015**, *5*, 7646. [[CrossRef](#)]
22. Zhang, J.; Du, P.; Xu, D.; Li, Y.; Peng, W.; Zhang, G.; Zhang, F.; Fan, X. Near-infrared responsive MoS<sub>2</sub>/Poly (N-isopropylacrylamide) hydrogels for remote light-controlled microvalves. *Ind. Eng. Chem. Res.* **2016**, *55*, 4526–4531. [[CrossRef](#)]
23. Lei, Z.; Zhou, Y.; Wu, P. Simultaneous exfoliation and functionalization of MoSe<sub>2</sub> nanosheets to prepare “Smart” nanocomposite hydrogels with tunable dual stimuli-responsive behavior. *Small* **2016**, *12*, 3112–3118. [[CrossRef](#)]
24. Xu, Q.; Zhao, S.; Deng, L.; Ouyang, J.; Wen, M.; Zeng, K.; Chen, W.; Zhang, L.; Liu, Y.-N. A NIR-II light responsive hydrogel based on 2D engineered tungsten nitride nanosheets for multimode chemo/photothermal therapy. *Chem. Commun.* **2019**, *55*, 9471–9474. [[CrossRef](#)]

25. Lin, L.; Ling, G.; Peng, F.; Zhang, F.; Jiang, S.; He, H.; Yang, D.; Zhang, P. Black phosphorus nanosheets and gemcitabine encapsulated thermo-sensitive hydrogel for synergistic photothermal-chemotherapy. *J. Colloid Interface Sci.* **2019**, *556*, 232–238.
26. Fabian, J.; Nakazumi, H.; Matsuoka, M. Near-infrared absorbing dyes. *Chem. Rev.* **1992**, *92*, 1197–1226. [[CrossRef](#)]
27. Phuong, P.T.M.; Jhon, H.; In, I.; Park, S.Y. Photothermal-modulated reversible volume transition of wireless hydrogels embedded with redox-responsive carbon dots. *Biomater. Sci.* **2019**, *7*, 4800–4812. [[CrossRef](#)] [[PubMed](#)]
28. Robby, A.I.; Lee, G.; Park, S.Y. NIR-induced pH-reversible self-healing monitoring with smartphone by wireless hydrogel sensor. *Sens. Actuator B Chem.* **2019**, *297*, 126783. [[CrossRef](#)]
29. Li, L.; Fu, L.; Ai, X.; Zhang, J.; Zhou, J. Design and fabrication of temperature-sensitive nanogels with controlled drug release properties for enhanced photothermal sterilization. *Chem. Eur. J.* **2017**, *23*, 18180–18186. [[CrossRef](#)]
30. Liu, C.; Ruan, C.; Shi, R.; Jiang, B.-P.; Ji, S.; Shen, X.-C. A near infrared-modulated thermosensitive hydrogel for stabilization of indocyanine green and combinatorial anticancer phototherapy. *Biomater. Sci.* **2019**, *7*, 1705–1715. [[CrossRef](#)]
31. Xia, L.-W.; Xie, R.; Ju, X.-J.; Wang, W.; Chen, Q.; Chu, L.-Y. Nano-structured smart hydrogels with rapid response and high elasticity. *Nat. Commun.* **2013**, *4*, 2226. [[CrossRef](#)]
32. Yang, J.; Choi, J.; Bang, D.; Kim, E.; Lim, E.-K.; Park, H.; Suh, J.-S.; Lee, K.; Yoo, K.-H.; Kim, E.-K.; et al. Convertible organic nanoparticles for near-infrared photothermal ablation of cancer cells. *Angew. Chem. Int. Ed.* **2011**, *50*, 441–444. [[CrossRef](#)]
33. Valdebenito, A.; Encinas, M.V. Thiophenols as chain transfer agents in the polymerization of vinyl monomers. *Polymer* **2005**, *46*, 10658–10662. [[CrossRef](#)]
34. Bongiovanni Abel, S.; Riberi, K.; Rivarola, C.R.; Molina, M.; Barbero, C.A. Synthesis of a smart conductive block copolymer responsive to heat and near infrared light. *Polymers* **2019**, *1*, 1744. [[CrossRef](#)]
35. Stejskal, J.; Sapurina, I. Polyaniline: Thin films and colloidal dispersions (IUPAC Technical Report). *Pure Appl. Chem.* **2005**, *77*, 815–826. [[CrossRef](#)]
36. Huang, J.; Kaner, R.B. A general chemical route to polyaniline nanofibers. *J. Am. Chem. Soc.* **2004**, *126*, 851–855. [[CrossRef](#)] [[PubMed](#)]
37. Woo, H.-Y.; Jung, W.-G.; Ihm, D.-W.; Kim, J.-Y. Synthesis and dispersion of polypyrrole nanoparticles in polyvinylpyrrolidone emulsion. *Synth. Met.* **2010**, *160*, 588–591. [[CrossRef](#)]
38. Bashkatov, A.N.; Genina, E.A.; Kochubey, V.I.; Tuchin, V.V. Optical properties of human skin, subcutaneous and mucous tissues in the wavelength range from 400 to 2000 nm. *J. Phys. D Appl. Phys.* **2005**, *38*, 2543. [[CrossRef](#)]
39. Wang, L.; Han, Y.; Huang, Y. Usage of conductive polymer composite as the object film of eddy current gap sensor. *IEEE Trans. Instrum. Meas.* **2013**, *62*, 3202–3208. [[CrossRef](#)]
40. Marsman, A.W.; Hart, C.M.; Gelinck, G.H.; Geuns, T.C.T.; de Leeuw, D.M. Doped polyaniline polymer fuses: Electrically programmable read-only-memory elements. *J. Mater. Res.* **2004**, *19*, 2057–2060. [[CrossRef](#)]
41. Pei, Q.; Qian, E. Protonation and deprotonation of polypyrrole chain in aqueous solutions. *Synth. Met.* **1991**, *45*, 35–48. [[CrossRef](#)]
42. Lai, H.; Wu, P. A infrared spectroscopic study on the mechanism of temperature-induced phase transition of concentrated aqueous solutions of poly (*N*-isopropylacrylamide) and *N*-isopropylpropionamide. *Polymer* **2010**, *51*, 1404–1412. [[CrossRef](#)]
43. Ashraf, S.; Park, H.-K.; Park, H.; Lee, S.-H. Snapshot of phase transition in thermoresponsive hydrogel PNIPAM: Role in drug delivery and tissue engineering. *Macromol. Res.* **2016**, *24*, 297–304. [[CrossRef](#)]
44. Abel, S.B.; Molina, M.A.; Rivarola, C.R.; Kogan, M.J.; Barbero, C.A. Smart polyaniline nanoparticles with thermal and photothermal sensitivity. *Nanotechnology*. **2014**, *25*, 495602. [[CrossRef](#)]
45. Kumar, A.; Mishra, R.; Reinwald, Y.; Bhat, S. Cryogels: Freezing unveiled by thawing. *Mater. Today* **2010**, *13*, 42–44. [[CrossRef](#)]
46. Molina, M.A.; Rivarola, C.R.; Miras, M.C.; Lescano, D.; Barbero, C.A. Nanocomposite synthesis by absorption of nanoparticles into macroporous hydrogels. Building a chemomechanical actuator driven by electromagnetic radiation. *Nanotechnology* **2011**, *22*, 5504. [[CrossRef](#)] [[PubMed](#)]

47. Bongiovanni Abel, S.; Molina, M.; Rivarola, C.R.; Barbero, C.A. A novel method to generate nanocomposites containing polypyrrole or polyaniline nanoparticles dispersed in a thermosensitive hydrogel matrix. Evidence of photothermal collapse under radiofrequency or microwave irradiation. *Polym. Chem.* **2019**. in review.
48. Lira, L.M.; Córdoba de Torresi, S.I. Conducting polymer–hydrogel composites for electrochemical release devices: Synthesis and characterization of semi-interpenetrating polyaniline–polyacrylamide networks. *Electrochem. Commun.* **2005**, *7*, 717–723. [[CrossRef](#)]
49. Siddhanta, S.K.; Gangopadhyay, R. Conducting polymer gel: Formation of a novel semi-IPN from polyaniline and crosslinked poly (2-acrylamido-2-methyl propanesulphonic acid). *Polymer* **2005**, *46*, 2993–3000. [[CrossRef](#)]
50. Molina, M.A.; Rivarola, C.R.; Barbero, C.A. Study on partition and release of molecules in superabsorbent thermosensitive nanocomposites. *Polymer* **2012**, *53*, 445–453. [[CrossRef](#)]
51. Erbil, C.; Saraç, A.S. Description of the turbidity measurements near the phase transition temperature of poly (N-isopropyl acrylamide) copolymers: The effect of pH, concentration, hydrophilic and hydrophobic content on the turbidity. *Eur. Polym. J.* **2002**, *38*, 1305–1310. [[CrossRef](#)]
52. Stile, R.A.; Healy, K.E. Poly (N-isopropylacrylamide)-Based Semi-interpenetrating Polymer Networks for Tissue Engineering Applications. 1. Effects of Linear Poly (acrylic acid) Chains on Phase Behavior. *Biomacromolecules* **2002**, *3*, 591–600. [[CrossRef](#)]
53. Pan, L.; Yu, G.; Zhai, D.; Lee, H.R.; Zhao, W.; Liu, N.; Wang, H.; Tee, B.C.K.; Shi, Y.; Cui, Y.; et al. Hierarchical nanostructured conducting polymer hydrogel with high electrochemical activity. *Proc. Natl. Acad. Sci. USA* **2012**, *10*, 9287–9292. [[CrossRef](#)]
54. Shi, Y.; Ma, C.; Peng, L.; Yu, G. Conductive “Smart” Hybrid Hydrogels with PNIPAM and Nanostructured Conductive Polymers. *Adv. Funct. Mater.* **2015**, *25*, 1219–1225. [[CrossRef](#)]
55. Huang, S.; MacDiarmid, A.G. Optical properties of polyaniline. *Polymer* **1993**, *34*, 1833–1845. [[CrossRef](#)]
56. Tao, Y.; Zhao, J.X.; Wu, C.X. Polyacrylamide hydrogels with trapped sulfonated polyaniline. *Eur. Polym. J.* **2005**, *41*, 1342–1349. [[CrossRef](#)]
57. Martínez, M.V.; Molina, M.; Barbero, C.A. Poly (N-isopropylacrylamide) Crosslinked Gels as Intrinsic Amphiphilic Materials. Swelling Properties Used to Build Novel Interphases. *J. Phys. Chem. B* **2018**, *122*, 9038–9048. [[CrossRef](#)] [[PubMed](#)]
58. Lanzalaco, S.; Armelin, E. Poly (N-isopropylacrylamide) and Copolymers: A Review on Recent Progresses in Biomedical Applications. *Gels* **2017**, *3*, 36. [[CrossRef](#)]
59. Martínez, M.V.; Bongiovanni Abel, S.; Rivero, R.; Miras, M.C.; Rivarola, C.R.; Barbero, C.A. Polymeric nanocomposites made of a conductive polymer and a thermosensitive hydrogel: Strong effect of the preparation procedure on the properties. *Polymer* **2015**, *78*, 94–103. [[CrossRef](#)]
60. Reghu, M.; Cao, Y.; Moses, D.; Heeger, A.J. Counterion-induced processibility of polyaniline: Transport at the metal-insulator boundary. *Phys. Rev. B* **1993**, *47*, 1758–1762. [[CrossRef](#)]
61. Martínez, M.V.; Molina, M.A.; Abel, S.B.; Barbero, C.A. Large Swelling Capacities of Crosslinked Poly (N-isopropylacrylamide) Gels in Organic Solvents. *MRS Adv.* **2018**, *3*, 3735–3740. [[CrossRef](#)]
62. Liu, Z.; Qi, D.; Guo, P.; Liu, Y.; Zhu, B.; Yang, H.; Liu, Y.; Li, B.; Zhang, C.; Yu, J.; et al. Thickness-Gradient Films for High Gauge Factor Stretchable Strain Sensors. *Adv. Mater.* **2015**, *27*, 6230–6237. [[CrossRef](#)]
63. Molina, M.; Asadian-Birjand, M.; Balach, J.; Bergueiro, J.; Miceli, E.; Calderon, M. Stimuli-responsive nanogel composites and their application in nanomedicine. *Chem. Soc. Rev.* **2015**, *44*, 6161–6186. [[CrossRef](#)]
64. Rivero, R.E.; Alustiza, F.; Rodríguez, N.; Bosch, P.; Miras, M.C.; Rivarola, C.R.; Barbero, C.A. Effect of functional groups on physicochemical and mechanical behavior of biocompatible macroporous hydrogels. *React. Funct. Polym.* **2015**, *97*, 77–85. [[CrossRef](#)]
65. Haque, M.A.; Kurokawa, T.; Gong, J.P. Super tough double network hydrogels and their application as biomaterials. *Polymer* **2012**, *53*, 1805–1822. [[CrossRef](#)]

